



# EMBRITTLMENT OF A 2205 DUPLEX STAINLESS STEEL IN THE TEMPERATURE RANGE OF 550-700°C

L. L. Martins\*, J. M. Albuquerque\*, T. Otárola† and A. Mateo†

\*Instituto de Soldadura e Qualidade, Oeiras, Portugal.

†Departament Ciència de los Materials e Ingeniería Metalúrgica, Universitat Politècnica de Catalunya, Barcelona, Spain.

## ABSTRACT

We investigated the effect of heat treatments on a 2205 Duplex Stainless Steel, performed in the range of 550-700°C with different exposure times and cooling rates. The hardness and impact toughness (Charpy V) of the aged specimens were measured while the corresponding microstructure was studied (optical microscopy and TEM). The results indicated that the steel is susceptible to embrittlement with increasing heat treatment time, temperature and decreasing cooling rate. A single type of phase transformation was identified only above 600°C 10H, furnace cooling. The morphology observed indicates the nucleation and growth of the Mo enriched phase,  $\chi$  phase,  $Fe_{36}Cr_{12}Mo_{12}$ . The work presented here is a part of a broad study on 2205's microstructure evolution under aging, pre-deformation, weldability, residual stress relief and corrosion resistance.

## INTRODUCTION

Duplex stainless steels (DSS's, consisting of two phases, ferrite and austenite, in roughly equal amounts) combine high mechanical properties with improved corrosion resistance, determining its wide application in the chemical, petrochemical industries, power plants and marine construction. However, they present technical limitations due to embrittlement, as a consequence of thermal cycles, such as those arising from manufacturing, welding or in-service of the components [1]. Aging conditions, excess alloying elements or pre-deformation lead to microstructure modifications (e.g. ferrite/austenite ratio) and second-phases precipitation (e.g.  $\sigma$  phase, carbides, nitrides), hindering the material's performance.

DSSs are characterized by two embrittlement temperature ranges (C-shaped curves) which exhibit several secondary phases ( $\sigma, \gamma_2, \chi, \pi, G$ , etc...), carbides and nitrides precipitation at different holding times, as shown in Fig. 1. The first critical temperature range is situated between 350°C and 500°C involving spinodal decomposition of the  $\alpha$  ferrite or the nucleation and growth of Ni-Si-Mo rich f.c.c. G phase. The second critical range lies between 500° and 1100°C, and it involves the formation of carbides ( $M_2C_3$  and  $M_{23}C_6$ ), nitrides ( $Cr_2N$  and  $\pi$ ), secondary austenite  $\gamma_2, \chi, R$ , and  $\sigma$  phases depending upon the steel composition and its thermal conditions [2].

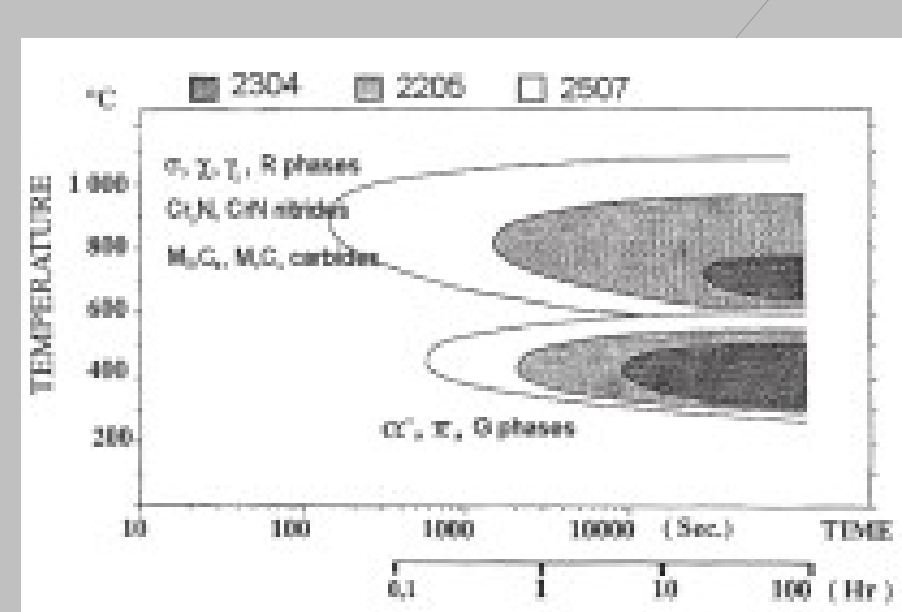


Figure 1. Typical TTT diagram of Duplex Stainless Steels

## EXPERIMENTAL RESULTS AND DISCUSSION

The heat treatments were performed in DSS 2205 plates (200x300x20 mm) supplied by Avesta, having the chemical composition reported in Tab. 1. Table 2 presents the different combinations for the 36 heat treatments performed in the range of 550-700°C, with the different exposure times and cooling rates.

| Element | C     | Si   | Mn   | Cr    | Ni   | Mo  | Cu  | N     |
|---------|-------|------|------|-------|------|-----|-----|-------|
| Wt%     | 0.015 | 0.40 | 1.43 | 22.39 | 5.69 | 3.2 | 0.2 | 0.183 |

Table 1. Chemical composition of duplex stainless steel 2205

| Temperature (°C) | Time (h) | Cooling condition |
|------------------|----------|-------------------|
| 550              | 1        | Air               |
| 600              | 3        | Furnace           |
| 650              | 10       | Water             |
| 700              | 10       | Water             |

Table 2. Heating cycles performed

Vickers macrohardness measurements were performed at room temperature, with a load of 10 Kg, in the as-received material on both the rolling (RD, plane XY) and transverse (TD, plane YZ) directions, Figure 2. Measurements were also performed, under the same conditions, for all the 36 heat treatments, Figure 3. Also standard Charpy-V specimens were machined along the rolling direction and the transversal direction. Impact tests were performed at 0, -40 and -80°C (Fig. 4) for both directions.

Hardness values reflect the as-received material strong anisotropy (Fig.2) as well as the important role of cooling rate. Despite the scatter (~10%) significant increase was found for samples subjected to slow cooling inside a furnace; the differences between air and water remaining relatively smaller (Fig.3). From the impact test results (Fig.4) an intense embrittlement is produced with increasing heat treatment time, temperature and decreasing cooling rate.

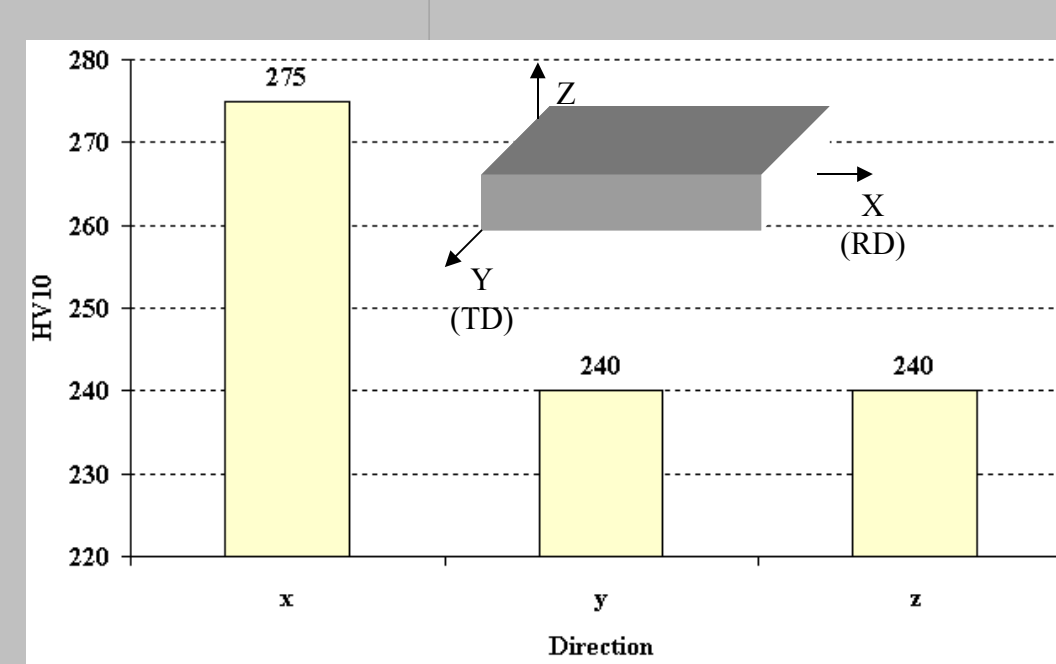


Figure 2. Hardness measurement results on base material

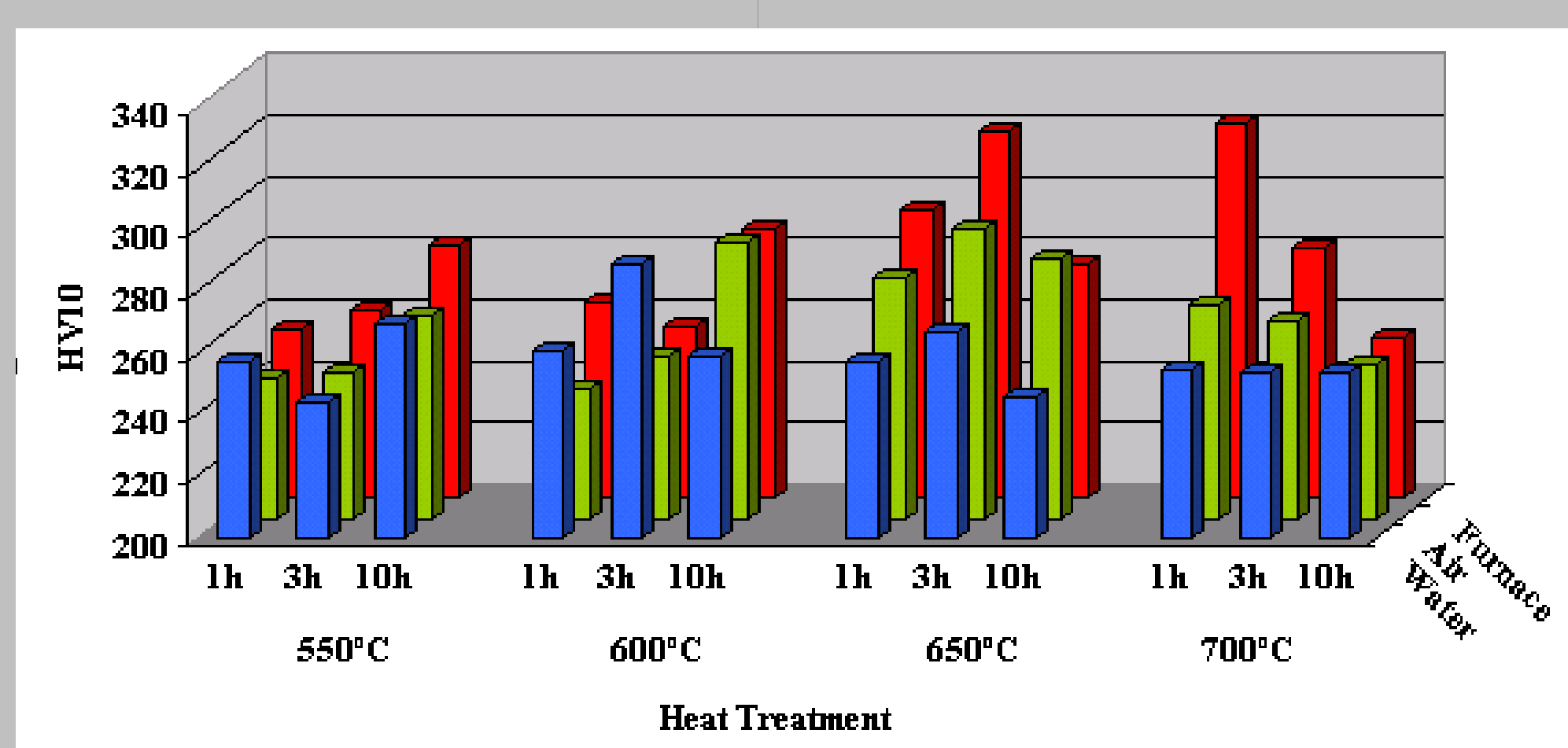


Figure 3. Hardness measurements on base material after heat treatment (rolling direction - RD)

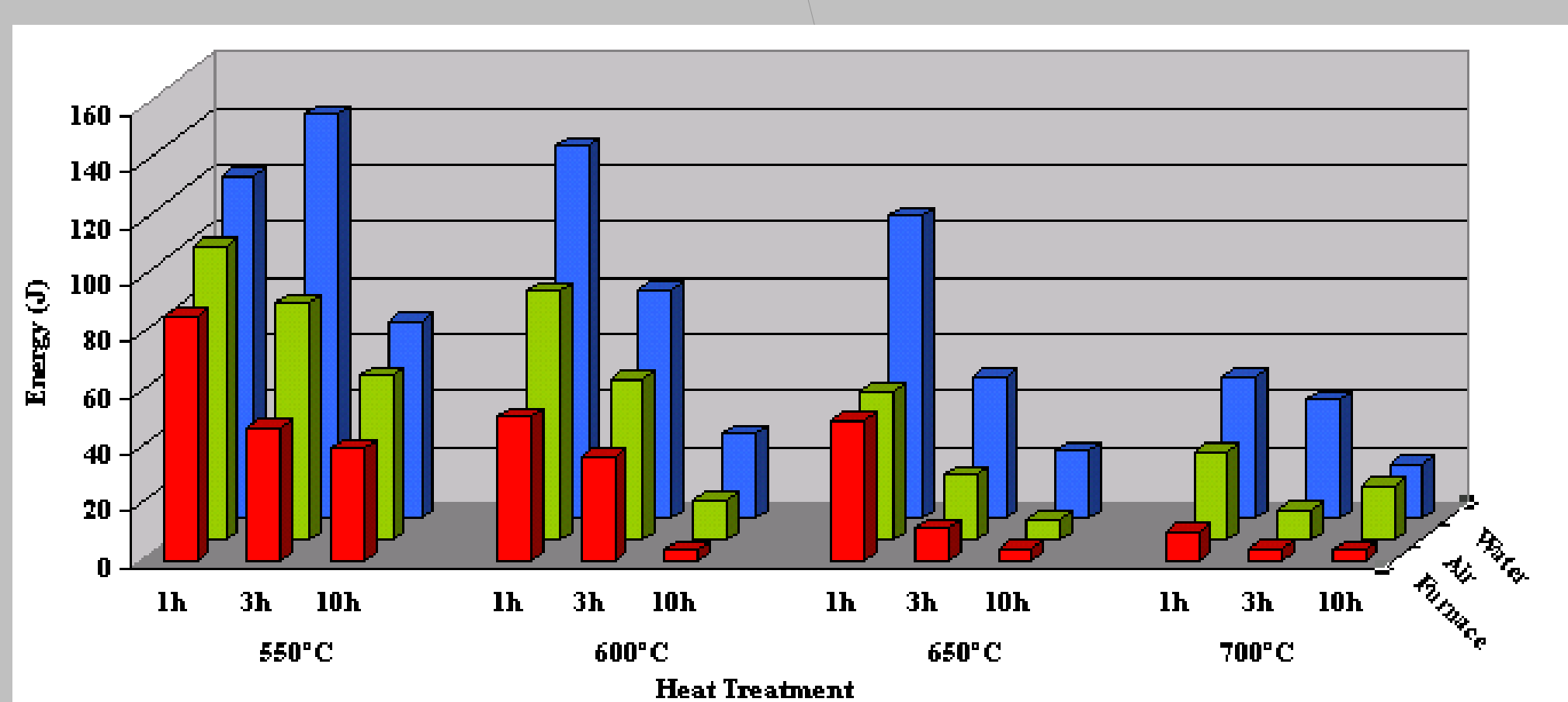


Figure 4. Impact tests results for base material with heat treatment. Test temperature: -80°C; Direction: RD

The microstructures of the aged specimens were observed under optical microscopy and are shown in Fig. 5 for 600°C and Fig. 6 for 700°C. Secondary particles are shown to precipitate in the grain boundaries and inside the ferrite phase. The ferrite content was measured by a Ferritoscope (Fig.7) and is shown to decrease slightly for higher temperatures, increasing times and decreasing cooling rates.

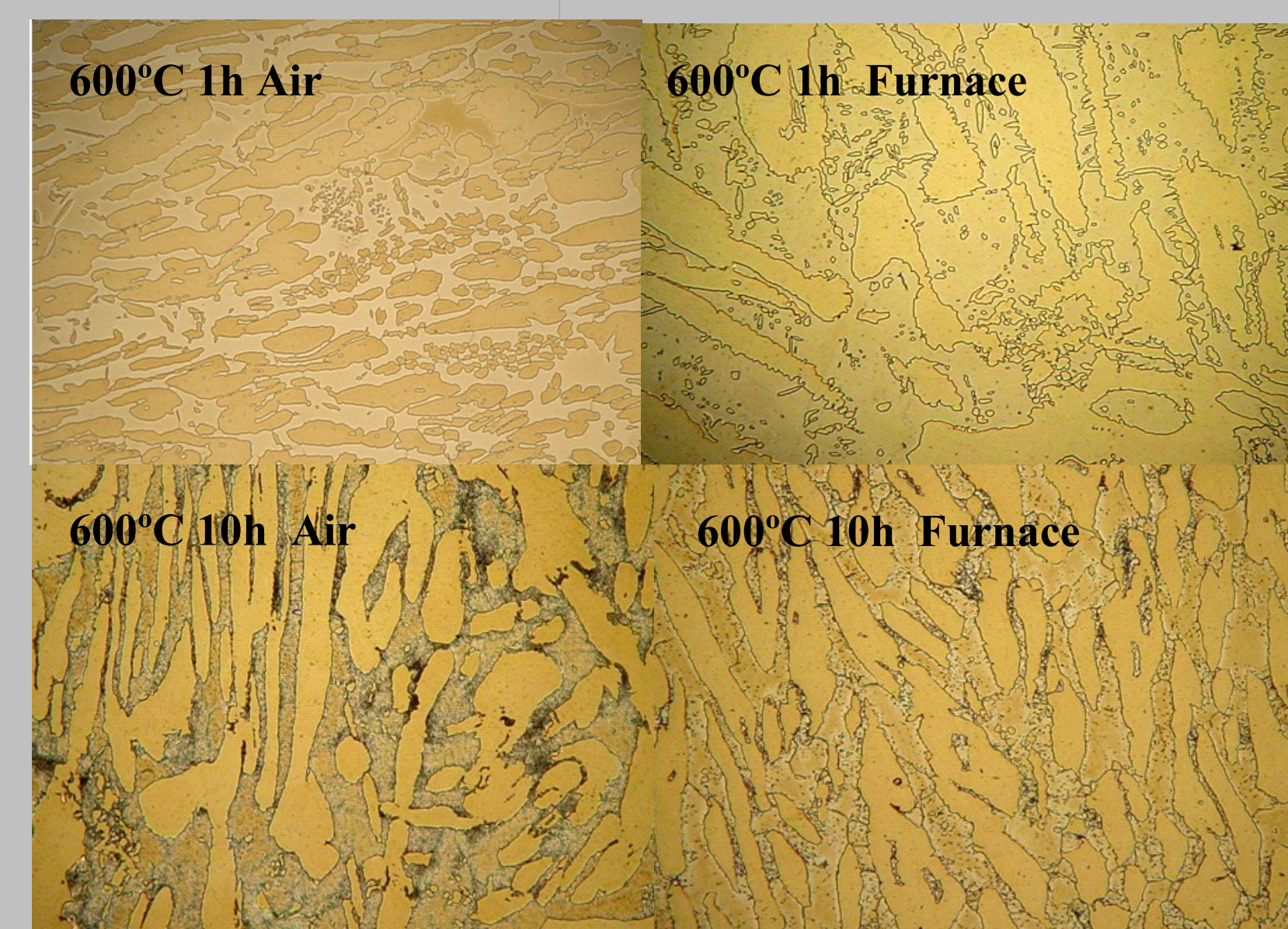


Figure 5. Optical microstructures from heat treated base material at 600°C with different aging times and cooling rates (200x)

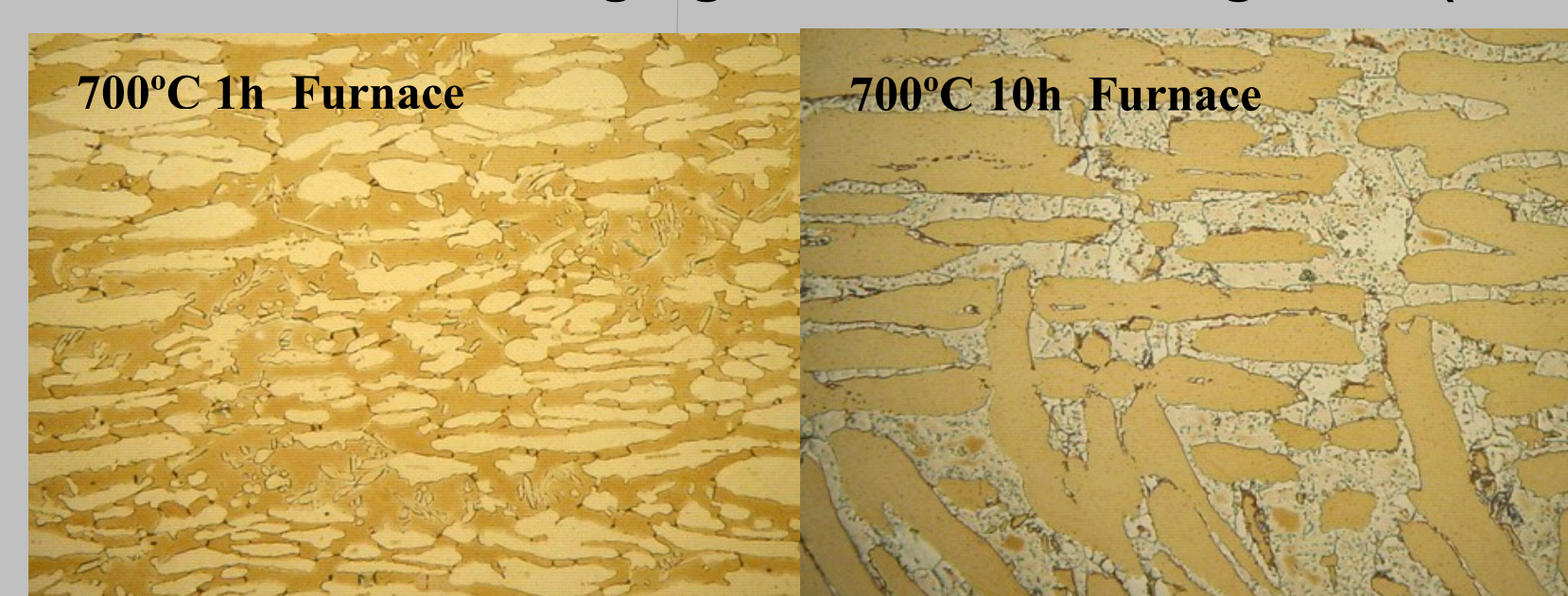


Figure 6. Optical microstructures from heat treated base material at 700°C with two different aging times and furnace cooling (200x)

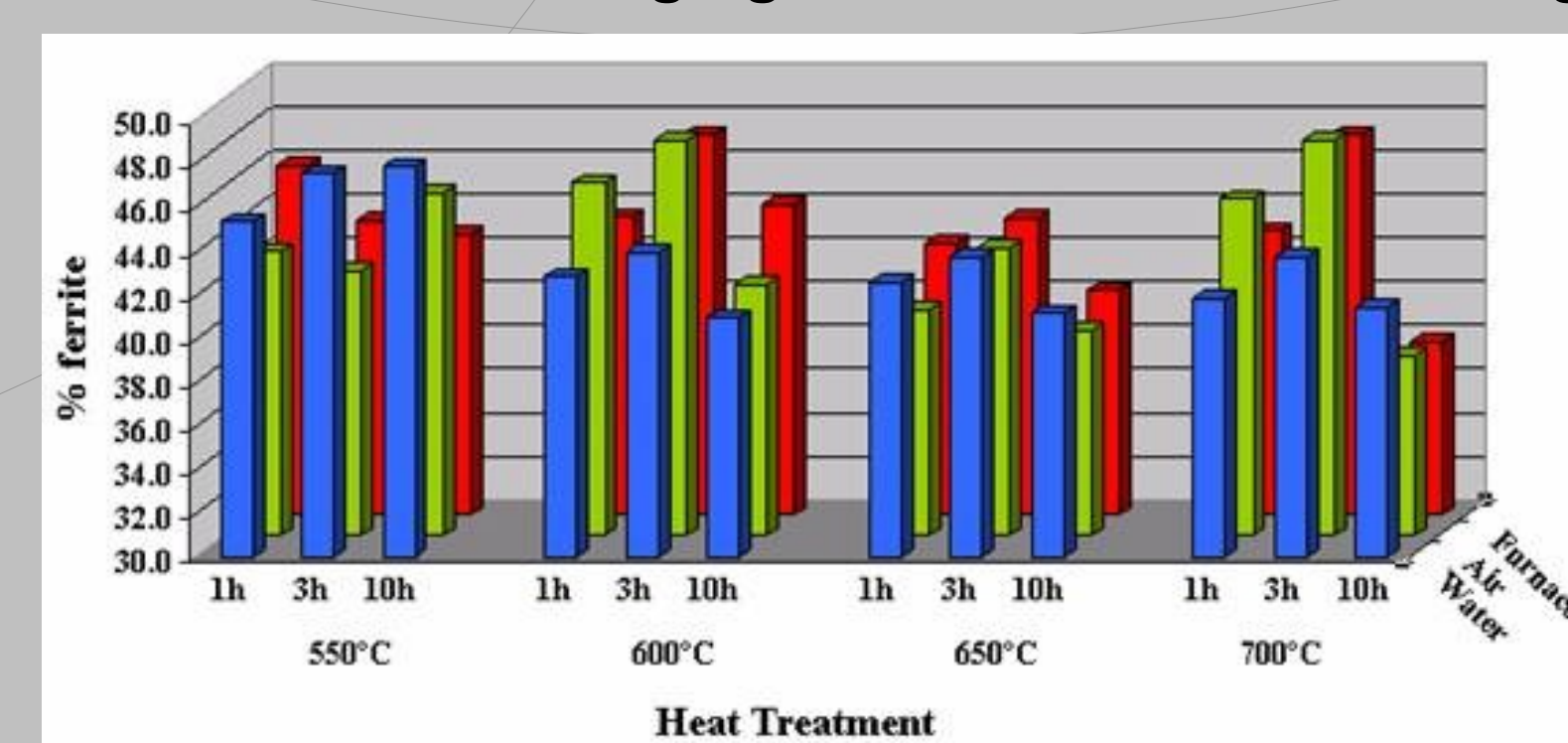


Figure 7. Ferrite content measured by ferritoscope after the heating cycles.

The influence of the thermal cycles was evaluated under TEM (Fig. 8). Six conditions were observed from a matrix of 3 temperatures (550, 600 and 700°C) and 2 exposure times (1 and 10 hours), furnace cooling. For all the conditions at 550°C no precipitation was found. At 600°C 10 H, a single type of phase transformation was identified: nucleation and growth of the  $\chi$  phase,  $Fe_{36}Cr_{12}Mo_{12}$ .

As shown in Fig.9 (a)  $\chi$  phase precipitates intergranularly and (Fig.9 (b)) intragranularly with a different orientation relationship from the classic cube-cube. The alignment of the precipitates in existence is not of the cubic-cubic symmetry but (110) $\delta$ //(-140) $\chi$  orientation relationship with the ferritic matrix, instead (Fig.9 (c)). It should be emphasized that  $\chi$  phase formation is less usual than that of  $\sigma$  phase, even though its temperature range are overlapped between 650°C and 900°C (along with  $Cr_2N$ ;  $M_{23}C_6$  precipitates, vd. Fig.1) [3].

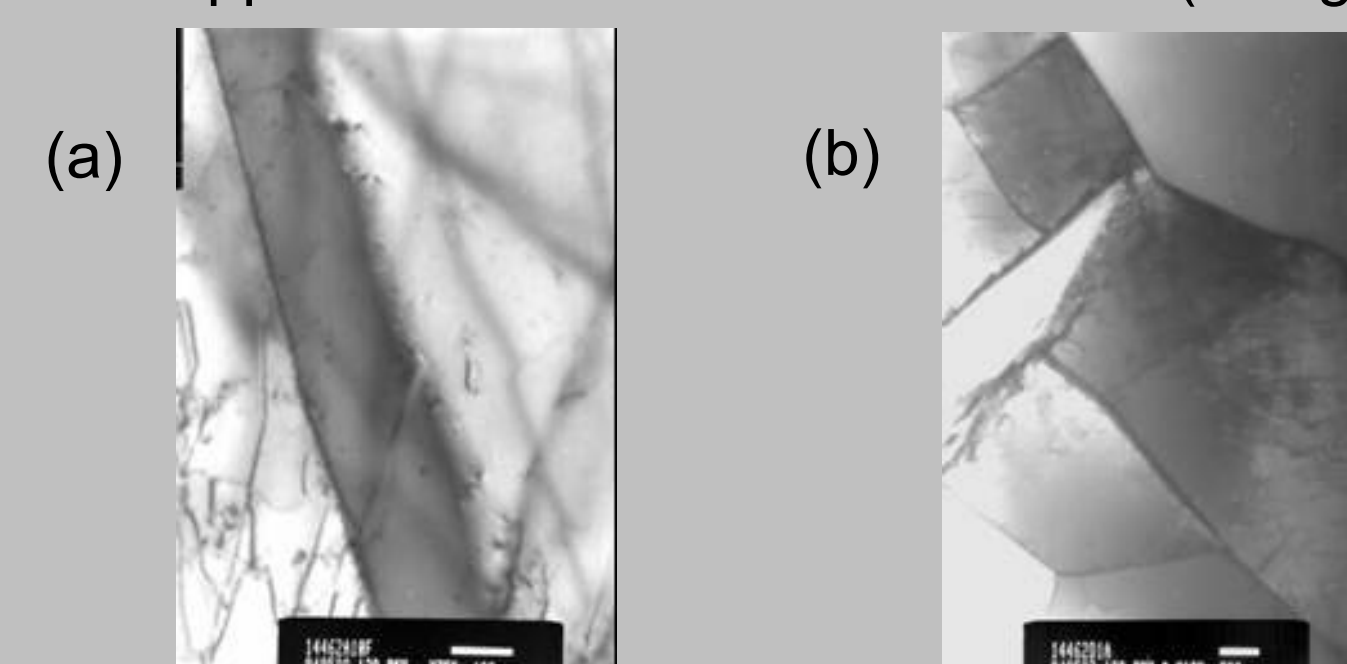


Figure 8. Microstructures from heat treated base material where is evident the absence of precipitation a) 550°C, 10 hours air cooling; b) 700°C, 1 hour air cooling.

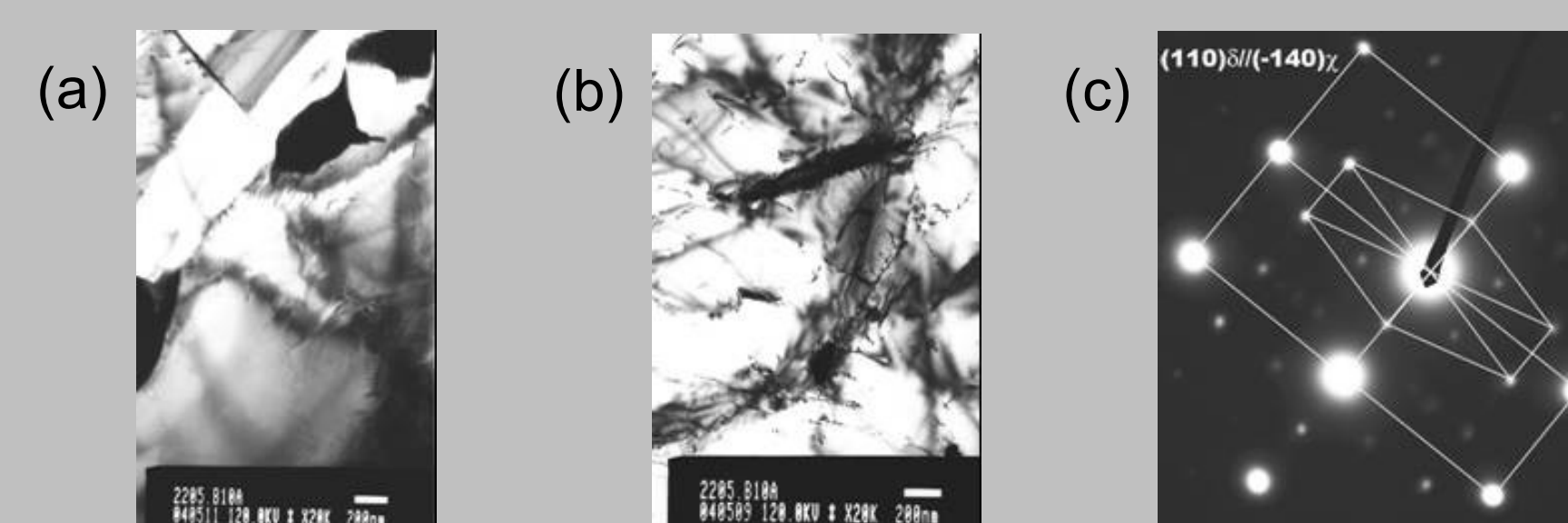


Figure 9. Evidence of Chi phase precipitation on heat treated base material with 10 hours exposure, 700°C furnace cooling a) intergranular  $\chi$  phase; b) intragranular  $\chi$  phase and c) diffraction pattern of intragranular  $\chi$  phase.

## CONCLUSIONS

- The temperature, the aging time increase and the decrease of cooling rate determine an increase of hardness and drop in toughness on DSS 2205.
- The aging schedules covered in this study did not induce a strong decrease in the amount of ferritic phase (less than 10% for the higher temperatures)
- A single type of phase transformation was only identified above 600°C 10H, furnace cooling. The morphology observed indicates the nucleation and growth of the Mo enriched phase,  $\chi$  phase,  $Fe_{36}Cr_{12}Mo_{12}$ .

## ACKNOWLEDGEMENTS

This investigation was developed with the financial support of the European Coal and Steel Research Programme (ECSC 7210-PR-365), involving partners ARCELOR INDUSTRIEL (FR);SIMR (SE), INASMET (ES), ISQ (PT), UPC (ES), AVESTA POLARIT (SE) and SANDVIK (SE).

## REFERENCES

- [1] T.H. Chen, K.L. Weng, and J.R. Yang, "The Effect of High-Temperature Exposure on the Microstructural Stability and Toughness Property in a 2205 Duplex Stainless Steel," *Mat. Sci. Eng. A338*, 259-270 (2002).
- [2] A. Redjajmia, G. Metauer, and G. Gantois, p.119 in "Proc Duplex Stainless Steel 91", vol.I, Beaune, France (1991).
- [3] K.L. Weng, T.H. Chen, and J.R. Yang, "The High-Temperature and Low-Temperature Aging Embrittlement in a 2205 Duplex Stainless Steel," *Bull. Coll. Eng., NTU*, (89) [10] 45-61 (2003).